PHYSICAL REVIEW A VOLUME 60, NUMBER 6 DECEMBER 1999

Contradiction of quantum mechanics with local hidden variables for quadrature phase measurements on pair-coherent states and squeezed macroscopic superpositions of coherent states

A. Gilchrist
Physics Department, University of Waikato, Hamilton, New Zealand

P. Deuar and M. D. Reid
Physics Department, University of Queensland, Brisbane, Australia

(Received 22 September 1998)

We demonstrate a contradiction of quantum mechanics with local hidden variable theories for continuous quadrature phase amplitude (''position'' and ''momentum'') measurements. A contradiction is shown possible for two quantum states: a pair-coherent state, and a superpositions of two coherent states, where the superposition state has been squeezed by the action of a two-mode squeezing operator. In one case a contradiction is still possible for states of increasing photon number, though the effect becomes smaller and more difficult to observe. The high efficiency of the homodyne method of measurement of quadrature phase amplitudes may open a way for a loophole-free test of local hidden variable theories, and the effect of detection loss on the contradiction with local hidden variables is calculated. [S1050-2947(99)02208-8]

PACS number(s): 03.65.Bz

I. INTRODUCTION

Einstein, Podolsky, and Rosen (EPR) [1] in 1935 presented an argument for the incompleteness of quantum mechanics. The argument was based on the validity of two premises: no action at a distance (locality) and realism. The original argument of EPR considered position and momentum measurements which could be performed on each of two particles at spatially separated locations. Bell [2] later showed that the predictions of quantum mechanics are incompatible with the premises of local realism (or local hidden variable theories). Experiments [3] based on Bell's result indicate the failure of local hidden variable theories.

Bell's original result, and subsequent theoretical (for example, Refs. [2,4–6]) and experimental work which test local hidden variable theories against quantum mechanics, considered measurements which have discrete outcomes, such as measurements of spin or photon number. By this we mean that the eigenvalues of the relevant system Hermitian operator, which represents the measurement in quantum mechanics, are discrete. The more successful experimental tests to date have involved photon counting measurements, for which the results of the measurement, a photon present or not, are discrete and only microscopically different. Associated with such experiments are relatively low detection efficiencies, which currently make a test of Bell's original inequality not feasible. These experiments test weaker inequalities [7] for which one needs to make additional auxiliary assumptions, preventing local hidden variable theories from being ruled out conclusively [8].

In this paper we expand on our initial results published previously [9]. We show how the predictions of quantum mechanics for certain entangled quantum superpositions of coherent states are in disagreement with those of local hidden variable theories for a situation involving continuous quadrature phase amplitude (''position'' and ''momentum'') measurements. By this we mean that the quantum predictions for the probability of obtaining results x and p for position and momentum (and various linear combinations of these coordinates) cannot be predicted by any local hidden variable theory.

This result is of fundamental interest since the original argument [1] of Einstein, Podolsky, and Rosen was given in terms of position and momentum measurements. It was pointed out by one of us [10] that quadrature phase amplitude measurements performed on the spatially separated outputs of the nondegenerate parametric amplifier could potentially be an example of the EPR paradox. A criterion was established to test for an EPR paradox even where correlations are not perfect, and ''elements of reality'' deduced using the premises of ''local realism'' (as defined originally by EPR) have an indeterminacy [11] in their values. Such EPR correlations, for continuous variables, were generated experimentally by Ou *et al.* [12] in a high efficiency experiment using homodyne detection. The original state considered by Einstein, Podolsky, and Rosen, however, and that produced experimentally in the realization by Ou *et al.*, give probability distributions for x and p completely compatible with local realism. This is so because, as discussed by Bell [2], the associated quantum Wigner distribution is positive in these cases and can thus provide a local hidden variable theory.

We also note that the homodyne method of measurement [13] of the quadrature phase amplitude employs a second ''local-oscillator'' field which combines with the original field to provide an amplification prior to photodetection. Large field fluxes fall incident on highly efficient photodiode detectors. This high intensity limit has not been indicated by previous works [14] which showed contradiction of quantum mechanics with local hidden variables using homodyne detection, since these analyses were restricted to a very low intensity of ''local-oscillator'' field. The possible macroscopic nature of such experiments has been discussed previ-

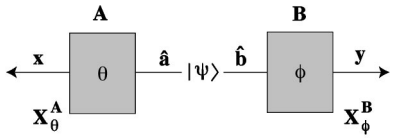

FIG. 1. Schematic representation of the proposed test of local hidden variables. Balanced homodyne detection allows measurement of the quadrature phase amplitudes X^A_θ and X^B_ϕ, to give results x and y, respectively.

ously [11] in the context of the Ou *et al.* realization of the Einstein-Podolsky-Rosen experiment. The high efficiency of detectors may also provide a way to test local hidden variables without the use of auxiliary assumptions which weaken the conclusions of the former photon counting measurements. We therefore calculate the effect of detection loss on the predicted contradiction with local hidden variables.

We stress that recent independent work by Yurke, Hillery, and Stoler [15] has also shown an incompatibility of quantum mechanics with local realism for quadrature phase amplitude measurements performed on certain quantum systems. There have also been further recent calculations by Munro and Milburn [16].

II. GENERAL FORMALISM

The Bell inequality is a consequence of the assumptions of locality and of realism. Consider an initial nondegenerate two-mode state $|\Psi\rangle$. Each mode of the state is directed to two physically separate locations A and B as indicated in Fig. 1.

Measurements are made of the field quadrature phase amplitudes X^A_θ at location A, and X^B_ϕ at location B. Here we define

$$X^A_\theta = \hat{a}\exp(-i\theta) + \hat{a}^\dagger \exp(i\theta),$$
$$X^B_\phi = \hat{b}\exp(-i\phi) + \hat{b}^\dagger \exp(i\phi). \tag{1}$$

Where our system is a harmonic oscillator, we note that the angle choices θ (or ϕ) equal to zero and $\pi/2$ will correspond to momentum and position measurements. The result for the amplitude measurement X^A_θ is a continuous variable which we denote by x (or sometimes x_θ). Similarly the result of the measurement X^B_ϕ is a continuous variable denoted by y (or sometimes x_ϕ).

We formulate a Bell inequality test for the experiment depicted by making the simplest possible binary classification of the continuous results x and y of the measurements. We classify the result of the measurement to be $+1$ if the quadrature phase result x (or y) is greater than or equal to zero, and -1 otherwise. With many measurements we build up the following probability distributions: $P^A_+(\theta)$ for obtaining a positive value of x; $P^B_+(\phi)$ for obtaining a positive y; and $P^{AB}_{++}(\theta,\phi)$ the joint probability of obtaining a positive result in both x and y. While this coarse-grain classification may not give as sensitive a test as a possible alternative Bell inequality derived for the continuous variables x and y directly, a violation found for the coarser treatment is still firm confirmation of failure of local realism for measurements with continuous variable outcomes (corresponding to a continuous eigenvalue spectrum in quantum mechanics).

If we now postulate the existence of a local hidden variable theory [2], we can write the probabilities $P_{\theta,\phi}(x,y)$ for getting a result x and y, respectively, upon the simultaneous measurements X^A_θ and X^B_ϕ in terms of the hidden variables λ as follows:

$$P_{\theta,\phi}(x,y) = \int \rho(\lambda) p^A_x(\theta,\lambda) p^B_y(\phi,\lambda) d\lambda. \tag{2}$$

The $\rho(\lambda)$ is the probability distribution for the hidden variable state denoted by λ, while $p^A_x(\theta,\lambda)$ is the probability of obtaining a result x upon measurement at A of X^A_θ, given the hidden variable state λ. The $p^B_y(\phi,\lambda)$ is defined similarly for the results and measurement at B. The independence of $p^A_x(\theta,\lambda)$ on ϕ, and $p^B_y(\phi,\lambda)$ on θ, is a consequence of the locality assumption that the measurement at A cannot be influenced by the experimenter's choice of parameter ϕ at the location B (and vice versa). It follows that the final measured probabilities $P^{AB}_{++}(\theta,\phi)$, $P^A_+(\theta)$, and $P^B_+(\phi)$ can be written in a similar form,

$$P^A_+(\theta) = \int \rho(\lambda) p^A_+(\lambda,\theta) d\lambda, \tag{3}$$

$$P^B_+(\phi) = \int \rho(\lambda) p^B_+(\lambda,\phi) d\lambda, \tag{4}$$

$$P^{AB}_{++}(\theta,\phi) = \int \rho(\lambda) p^A_+(\lambda,\theta) p^B_+(\lambda,\phi) d\lambda, \tag{5}$$

where we have simply set $p^A_+(\theta,\lambda) = \int_{x\geq 0} p^A_x(\theta,\lambda) dx$, and similarly for $p^B_+(\phi,\lambda)$. It is well known that one can now deduce [2] the following ''strong'' Clauser-Horne-Bell inequality (no auxiliary assumptions [7] have been made):

$$S = \frac{P^{AB}_{++}(\theta,\phi) - P^{AB}_{++}(\theta,\phi') + P^{AB}_{++}(\theta',\phi) + P^{AB}_{++}(\theta',\phi')}{P^A_+(\theta') + P^B_+(\phi)} \leq 1. \tag{6}$$

III. VIOLATION OF THE CLAUSER-HORNE-BELL INEQUALITY USING QUADRATURE PHASE MEASUREMENTS FOR A PAIR-COHERENT STATE

We consider the following two-mode entangled quantum superposition state, discussed originally by Agarwal and Tara and Agarwal [17,18] and also Reid and Krippner [19]:

$$|\Psi\rangle_m = \mathcal{N}\int_0^{2\pi} e^{-im\varsigma} |r_0 e^{i\varsigma}\rangle_a |r_0 e^{-i\varsigma}\rangle_b d\varsigma. \tag{7}$$

Here $\mathcal{N}$ is a normalization coefficient. Here $|\ldots\rangle_a$ and $|\ldots\rangle_b$ are coherent states in modes $\hat{a}$ and $\hat{b}$, where the $\hat{a}^\dagger$ and $\hat{a}$, and $\hat{b}^\dagger$ and $\hat{b}$ are the usual boson operators for the two spatially separated systems (for example, field modes) at locations A and B, respectively. In many optical systems the $\hat{a}$ and $\hat{b}$ are referred to as the signal and idler fields, respectively. This state, originally defined and considered by Agar-

wal and termed a pair-coherent state, is an eigenstate of the photon number difference between signal and idler modes, with eigenvalue m:

$$(\hat{a}^\dagger\hat{a}-\hat{b}^\dagger\hat{b})|\Psi\rangle_m = m|\Psi\rangle_m . \tag{8}$$

Also it is an eigenstate of the operator $\hat{a}\hat{b}$,

$$\hat{a}\hat{b}|\Psi\rangle_m = r_0^2|\Psi\rangle_m . \tag{9}$$

For our purposes we shall concentrate on the $m=0$ case in Eq. (7) which when normalized is

$$|\Psi\rangle = \mathcal{B}^{1/2}\int_0^{2\pi}|r_0e^{i\varsigma}\rangle_a|r_0e^{-i\varsigma}\rangle_b d\varsigma, \tag{10}$$

with

$$\mathcal{B}^{-1} = 4\pi^2 e^{-2r_0^2} I_0(2r_0^2), \tag{11}$$

and where I_0 is a modified Bessel function. Expanding out each of the coherent states into number states $|n\rangle$ for each mode we can write the state as

$$|\Psi\rangle = [I_0(2r_0^2)]^{-1/2}\sum_{n=0}^{\infty}\frac{(r_0^2)^n}{n!}|n\rangle_a|n\rangle_b , \tag{12}$$

as originally introduced by Agarwal.

The quantum state given by Eqs. (10) and (12) is potentially generated, from vacuum fields, by the interaction modeled by the following Hamiltonian, in which coupled signal-idler loss dominates over linear single-photon loss.

$$H = i\hbar E(\hat{a}^\dagger\hat{b}^\dagger-\hat{a}\hat{b})+\hat{a}\hat{b}\hat{\Gamma}^\dagger+\hat{a}^\dagger\hat{b}^\dagger\hat{\Gamma}. \tag{13}$$

This interaction is achievable in principle by nondegenerate parametric oscillation [19] in a limit where uncorrelated single-photon loss in each of the signal and idler fields becomes negligible. Here E represents a coherent driving parametric term which generates signal-idler pairs, while $\hat{\Gamma}$ represents reservoir systems which give rise to the coupled signal-idler loss. The Hamiltonian preserves the signal-idler photon number difference $\hat{a}^\dagger\hat{a}-\hat{b}^\dagger\hat{b}$, of which the quantum state (10) is an eigenstate, with eigenvalue zero. We note the analogy here to the single-mode ''even'' and ''odd'' [20] coherent superposition states

$$N_\pm^{1/2}(|\alpha\rangle\pm|-\alpha\rangle) \tag{14}$$

(where α is real and $N_\pm^{-1}=2[1\pm\exp(-2|\alpha|^2)]$) which are generated [21,22] by the degenerate form (set $\hat{a}=\hat{b}$) of the Hamiltonian equation (13) and which have been recently experimentally generated [23]. These states are of interest in that they resemble, for large α, ''Schrödinger-cat''states [24].

The calculation of the quantum prediction for S for the quantum state (10) is straightforward in principle. We use

$${}_a\langle x_\theta|\alpha\rangle_a = \left(\frac{1}{2\pi}\right)^{1/4} \times\exp\left\{-\frac{1}{4}x_\theta^2+\alpha e^{-i\theta}x_\theta-\frac{1}{2}\alpha^2e^{-2i\theta}-\frac{1}{2}|\alpha|^2\right\}, \tag{15}$$

where $|x_\theta\rangle_a$ is the eigenstate of $X_\theta^A=\hat{a}\exp(-i\theta)+\hat{a}^\dagger\exp(i\theta)$, and we use similar definitions for mode $\hat{b}$. We have

$$\begin{aligned}{}_a\langle x_\theta|_b\langle x_\phi|\Psi\rangle &= \mathcal{B}^{1/2}\int_0^{2\pi}d\varsigma\,{}_a\langle x_\theta|_b\langle x_\phi|r_0e^{i\varsigma}\rangle_a|r_0e^{-i\varsigma}\rangle_b \\ &= \left(\frac{\mathcal{B}}{2\pi}\right)^{1/2}\exp\{-r_0^2\} \times\exp\left\{-\frac{1}{2}(x_\theta^2+x_\phi^2)\right\}\int_0^{2\pi}d\vartheta \\ &\quad\times\exp\left\{-\frac{r_0^2}{2}(e^{2i(\vartheta-\chi)}+e^{-2i\vartheta})\right\},\end{aligned} \tag{16}$$

where $\vartheta=\varsigma+\phi$, $\chi=\theta+\phi$. The probability distribution $P_{\theta,\phi}(x_\theta,x_\phi)$ becomes

$$\begin{aligned}P_{\theta,\phi}(x_\theta,x_\phi) &= |{}_A\langle x_\theta|_B\langle x_\phi|\Psi\rangle|^2 \\ &= \frac{\mathcal{B}}{2\pi}\exp\left\{-\frac{1}{2}(x_\theta^2+x_\phi^2)\right\}\int_0^{2\pi}d\vartheta\int_0^{2\pi}d\vartheta' \\ &\quad\times\exp\{-\sqrt{2}[A(r_0)x_\theta+B(r_0)x_\phi]+C(r_0)\},\end{aligned} \tag{17, 18}$$

with the factors

$$A(r_0) = -\frac{r_0}{\sqrt{2}}(e^{i(\vartheta-\chi)}+e^{-i(\vartheta'-\chi)}),$$

$$B(r_0) = -\frac{r_0}{\sqrt{2}}(e^{-i\vartheta}+e^{i\vartheta'}),$$

$$C(r_0) = -\frac{r_0^2}{2}(4+e^{2i(\vartheta-\chi)}+e^{-2i(\vartheta'-\chi)}+e^{-2i\vartheta}+e^{2i\vartheta'}).$$

It is evident from this expression that $P_{\theta,\phi}(x_\theta,x_\phi)$ is a function only of the angle sum $\chi=\theta+\phi$ so we can abbreviate $P_{++}^{AB}(\theta,\phi)=P_{++}^{AB}(\chi)$. Also we see that on making the variable change $\eta=-\vartheta$ and $\eta'=-\vartheta'$ in the integrations (18), we obtain the same form for the expression $P_{\theta,\phi}(x_\theta,x_\phi)$ but replacing χ with $-\chi$. That is, we have $P_{++}^{AB}(\chi)=P_{++}^{AB}(-\chi)$.

We note that the probabilities $P_{\theta,\phi}(x,y)$ for the pair-coherent state could also be evaluated using the expression (12). Here one uses the result

$$\langle x_\theta|n\rangle = \frac{1}{\sqrt{2^n n!}}\left(\frac{1}{2\pi}\right)^{1/4}e^{-x_\theta^2/4}e^{-ni\theta}H_n\left(\frac{1}{\sqrt{2}}x_\theta\right). \tag{19}$$

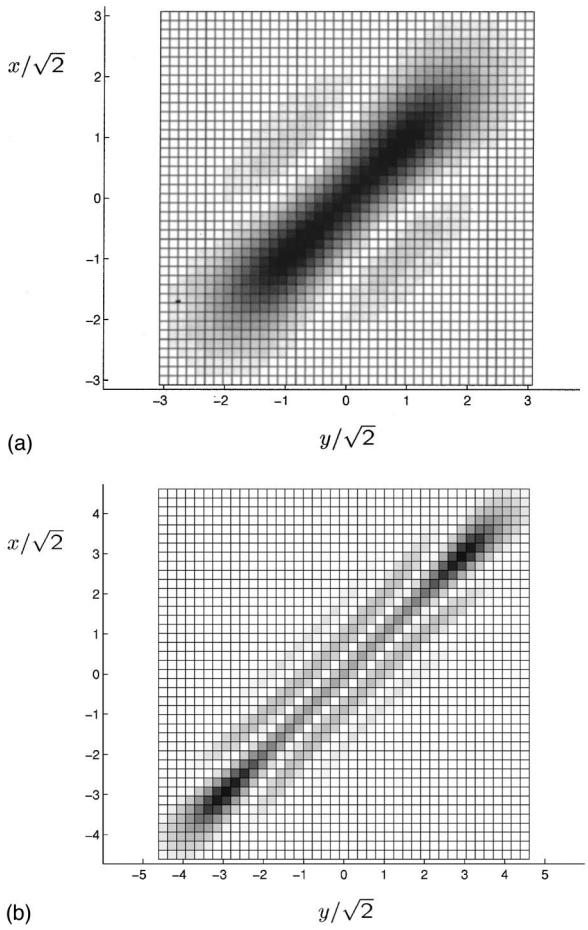

FIG. 2. Representation of the probability $P_{\theta,\phi}(x,y)$ for getting a result x and y, respectively, upon the simultaneous measurements X^A_θ and X^B_ϕ, where $\theta=-\phi$. (a) $r_0=1.1$; (b) $r_0=2.5$ showing the increasing separation of peaks and the interference fringes characteristic of quantum superposition states.

This approach was used by Tara and Agarwal [18], who calculated $P_{\theta,\phi}(x,y)$ in a paper to establish the existence of correlations between the quadrature phase amplitudes X^A_θ and X^B_ϕ at the locations A and B, respectively. Tara and Agarwal [18] showed the correlation to be sufficient to satisfy the criterion developed by one of us (Reid [10]) for a demonstration of the Einstein-Podolsky-Rosen paradox. As discussed in the Introduction and explained elsewhere, the existence of such correlations does not in itself imply a failure of local realism.

Figure 2 shows the distribution $P_{\theta,\phi}(x,y)$ for selected choices of r_0 and $\theta+\phi$. The strong correlation for $\theta=-\phi$ is evident.

We proceed to calculate the event probabilities needed for the Clauser-Horne- (CH) Bell inequality (6). We have

$$P^{AB}_{++}(\theta,\phi)=\int_0^\infty dx_\phi \int_0^\infty dx_\theta P_{\theta,\phi}(x_\theta,x_\phi),$$

$$P^{A}_{+}(\theta)=\int_{-\infty}^\infty dx_\phi \int_0^\infty dx_\theta P_{\theta,\phi}(x_\theta,x_\phi), \tag{20}$$

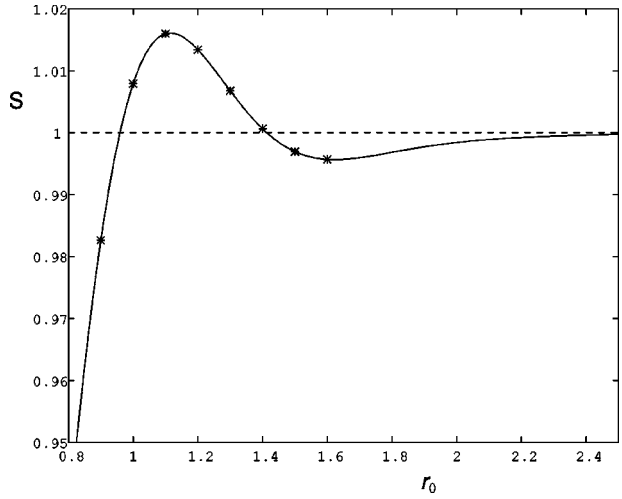

FIG. 3. Plot of S versus r_0, for the angle values indicated in the text: $\delta_1=\delta_2=\delta=\pi/2$ and $\sigma=5\pi/4$.

$$P^{B}_{+}(\phi)=\int_{-\infty}^\infty dx_\theta \int_0^\infty dx_\phi P_{\theta,\phi}(x_\theta,x_\phi).$$

These integrations could be evaluated by direct numerical integration [use Eqs. (16) and (17) directly]. An analysis allowing for a much quicker numerical evaluation is presented in Appendix A.

We note certain properties of the distribution $P^{AB}_{++}(\theta,\phi)$: $P^{AB}_{++}(\theta,\phi)=P^{AB}_{++}(\chi)$; $P^{AB}_{++}(\chi)=P^{AB}_{++}(\chi+2\pi)$; $P^{AB}_{++}(\chi)=P^{AB}_{++}(-\chi)$; and the marginals satisfy, as proved rigorously in Appendix A, $P^A_+(\theta)=P^B_+(\phi)=0.5$. It then becomes apparent that the value for S involves only three independent angles [which we specify by $\delta_1=\theta-\theta'$, $\delta_2=\phi'-\phi$, $\sigma=-(\theta+\phi')$].

Results for S are shown in Fig. 3, for the choice of measurement angles giving $\delta_1=\delta_2=\delta=\pi/2$ and $\sigma=-3\pi/4$ (or the negative values $\delta=-\pi/2$ and $\sigma=3\pi/4$). This choice corresponds to $\theta+\phi=\theta'+\phi'=-(\theta'+\phi)=\pi/4$, $\theta+\phi'=3\pi/4$ (for example set $\theta=0$, $\phi=-\pi/4$, $\theta'=\pi/2$, and $\phi'=-3\pi/4$) so that the simplification $S=3P^{AB}_{++}(\pi/4)-P^{AB}_{++}(3\pi/4)$ can be made. We have shown that for small r_0 (less than about 1.5) this angle choice maximizes S. Figures 4 and 5 illustrate the variation in the value of S with variation in choice of angles.

Violations of the Bell inequality, and hence contradiction with the predictions of local hidden variables, are indicated for $0.96\lesssim r_0\lesssim 1.41$, the maximum violation of $S\approx 1.0161$ being around $r_0\approx 1.12$. We note that this approximate value of r_0 was also found by Tara and Agarwal [18] to be optimal for the demonstration of EPR correlations, and corresponds to the greatest amount of two-mode squeezing. We have mentioned previously in the Introduction, however, that the existence of such correlations does not imply necessarily a violation of local realism for the experimental arrangement we consider in this paper.

We note that the violations are lost at larger coherent amplitudes r_0. It is possible to obtain (Appendix B) asymptotic (large r_0) analytical forms for the probability distributions which allow a complete search for all angles. Results indicate no violations of the Bell inequality (6) are possible.

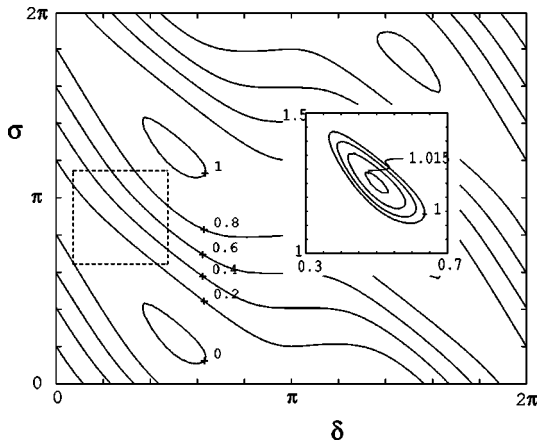

FIG. 4. For $r_0=1.1$ we show a contour plot of S as a function of σ and δ. The inset has units of π on its axis and shows a closeup of the region of violation denoted in the dashed square. Note the same violations occur for the lower square at $\delta=3\pi/2$ and $\sigma=3\pi/4$.

In the larger r_0 limit the probability distributions for x and y begin to show two widely separated peaks (as indicated by Fig. 2). For our particular choice of quantum state (the pair coherent state) the $+1$ and -1 results will never be truly macroscopically distinct because there is always a nonzero probability for values of x near zero. Nevertheless we hypothetically consider a situation where the $+1$ and -1 results of the measurement correspond to macroscopically distinct outcomes, resembling the ''alive'' and ''dead'' states of the ''Schrödinger cat.'' This is the truly macroscopic limit stressed by Leggett and Garg [25]. In fact it can be demonstrated that, for any quantum state, the incompatibility with local hidden variables must become increasingly small, for the case where the quadrature phase amplitude results x and y only take on values increasingly macroscopically distinct. In this limiting case, the addition of a noise term of order the standard quantum limit (this corresponds to a variance $\Delta^2 x=1$) to the result of quadrature phase amplitude measurement will not alter the $+1$ or -1 classification of the result. Yet it can be shown that the quantum predictions for the results of such a noisy experiment are given by the convolution of the quantum Wigner function $W(x_0^A,x_{\pi/2}^A,x_0^B,x_{\pi/2}^B)$ for the state (10), with the Gaussian noise term $(1/4\pi^2)\times\exp(-[x_0^{A2}+x_{\pi/2}^{A\,2}+x_0^{B2}+x_{\pi/2}^{B\,2}]/2)$. This new Wigner function is always positive (see, for example, Ref. [26]) and can then act as a local hidden variable theory which gives all the quantum predictions in the truly macroscopic ''dead'' or ''alive'' classification limit.

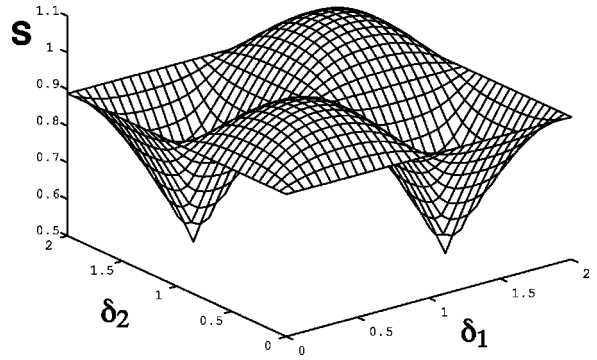

FIG. 5. Plot of the variation of the maximum value of S (optimizing with respect to σ) versus δ_1 and δ_2. Here $r_0=1.1$.

Accurate quadrature phase amplitude measurements have been performed in a now significant number of squeezed-state experiments, in which the measurement is performed using homodyne detection. This technique employs a local-oscillator field to create an amplification prior to detection, which means that fields of large intensity fall on the photodetectors. The method employs photodiode detectors and is more highly efficient than detection (see, for example, Ref. [27]) in the photon counting experiments which have characterized tests of Bell inequalities so far. These previous experiments are limited by detection efficiencies to the extent that no strong Bell inequality test has been performed to date. Given the efficiency of the homodyne detection method then, the smallness of the violation for the experiment proposed in this paper is not necessarily an indication of a relative lack of feasibility.

We then proceed to examine the effect of loss, such as from nonideal detectors, on the violations of the strong Bell inequalities.

IV. EFFECT OF DETECTION INEFFICIENCIES AND LOSS

It is well known that a nonideal photon detector can be modeled by a beam splitter followed by an ideal detector [13]. The attenuating beam splitter mixes our input signal mode operator $\hat{a}$ with the vacuum operator $\hat{a}_{\rm vac}$ to give two outputs $\hat{c}_A$ and $\hat{d}_A$ at location A:

$$\hat{c}_A=\sqrt{\eta}\hat{a}+\sqrt{1-\eta}\hat{a}_{\rm vac},$$
$$\hat{d}_A=\sqrt{1-\eta}\hat{a}-\sqrt{\eta}\hat{a}_{\rm vac}, \tag{21}$$

where η is the overall efficiency factor. The measured quadrature phase operator is now that of $\hat{c}_A$. With two spatially separated beam splitters modeling loss at each detector we may write our total input state as

$$|{\rm in}\rangle=\mathcal{B}^{1/2}\int_0^{2\pi}|r_0e^{i\varsigma}\rangle_a|0\rangle_{a_{\rm vac}}|r_0e^{-i\varsigma}\rangle_b|0\rangle_{b_{\rm vac}}d\varsigma, \tag{22}$$

where the $|0\rangle$ represent the vacuum inputs for input modes $a_{\rm vac}$ and $b_{\rm vac}$ to the two beam splitters. Using techniques outlined in Yurke and Stoler [28], one writes the output state as

$$|{\rm out}\rangle=\mathcal{B}^{1/2}\int_0^{2\pi}|\sqrt{\eta}r_0e^{i\varsigma}\rangle_{c_A}|\sqrt{1-\eta}r_0e^{i\varsigma}\rangle_{d_A}$$
$$\times|\sqrt{\eta}r_0e^{-i\varsigma}\rangle_{c_B}|\sqrt{1-\eta}r_0e^{-i\varsigma}\rangle_{d_B}d\varsigma. \tag{23}$$

The final probability of observing results x_θ and x_ϕ for the quadrature phase amplitude measurements in attenuated modes c_A and c_B is

$$P_{\theta,\phi}(x_\theta,x_\phi)=\int_{-\infty}^{+\infty}dx_{\mathrm{vac},\theta}\int_{-\mathrm{inf}}^{+\mathrm{inf}}dx_{\mathrm{vac},\phi}\times\left|{}_{c_A}\langle x_\theta|_{d_A}\langle x_{\mathrm{vac},\theta}|_{c_B}\langle x_\phi|_{d_B}\langle x_{\mathrm{vac},\phi}|\mathrm{out}\rangle\right|^2, \tag{24}$$

where we use Eq. (15) to calculate the probability amplitude. Calculation of the Gaussian integrals [use $\int d^2x\exp(-\lambda|x|^2+\mu x^*+\nu x)=(\pi/\lambda)\exp(\mu\nu/\lambda)$ which is valid for any μ or ν and $\mathrm{Re}\,\lambda>0$] in $x_{\mathrm{vac},\theta}$ and $x_{\mathrm{vac},\phi}$ and simplification gives the following modification of Eq. (18):

$$P_{\theta,\phi}(x_\theta,x_\phi)=\frac{\mathcal{B}}{2\pi}\exp\left(-\frac{1}{2}(x_\theta^2+x_\phi^2)\right)\int_0^{2\pi}d\vartheta\int_0^{2\pi}d\vartheta'\times\exp\{-\sqrt{2}[A(\sqrt{\eta}r_0)x_\theta+B(\sqrt{\eta}r_0)x_\phi]+C(\sqrt{\eta}r_0)\}\times\exp\{2(1-\eta)r_0^2\cos\vartheta-\vartheta'\}. \tag{25}$$

Following the calculation in Appendix A finally gives the marginals 1/2 as before and the expression $P_{\theta,\phi}(x_\theta,x_\phi)$ unchanged except that $k=-\sqrt{\eta}r_0/\sqrt{2}$ in Eq. (A15).

Calculations reveal violations to be negligible for $\eta\sim0.95$. Such high efficiencies may be achievable with homodyne detection. However, the sensitivity to loss, also noticed in the observation of fringes due to quantum ''Schrödinger-cat'' states [28], indicates that the limiting factor may well be the difficulty in the preparation of the quantum state.

V. TWO-MODE ''SCHRÖDINGER-CAT'' STATES

In this section we look at the possibility of violating the inequality (6) with the following superposition of two-mode coherent states (dropping explicit reference to the two modes for brevity):

$$|\mathrm{cat}\rangle=\mathcal{A}^{1/2}(|\boldsymbol{\alpha_0}\rangle+e^{i\varphi}|-\boldsymbol{\alpha_0}\rangle), \tag{26}$$

where $|\boldsymbol{\alpha_0}\rangle=|\alpha_0\rangle_a|\beta_0\rangle_b$ and $|\alpha_0\rangle_a$ is a coherent state in the mode $\hat{a}$. The normalization is given by

$$\mathcal{A}^{-1}=2(1+e^{-2(|\alpha_0|^2+|\beta_0|^2)}\cos\varphi). \tag{27}$$

Where the values of α_0,β_0 are large this state becomes a superposition of states macroscopically distinct in phase space and thus resembles the Schrödinger-cat state. There has been much discussion of the single-mode versions, Eq. (14), of this state, and recent experimental developments [23]. Multimode even-odd coherent states were studied in [29].

Both the EPR argument and the Bell inequalities make an assumption of locality and hence we need to make measurements at two distinct locations, distant from each other. To this end we have generalized the single-mode cat state (14) to two modes which are separated as indicated in Fig. 1.

We note that the two-mode cat state can be generated in principle by passing a single-mode ''cat'' state (14),

$$N^{1/2}(|\alpha\rangle+e^{i\varphi}|-\alpha\rangle) \tag{28}$$

(where α is real and $N^{-1}=2[1+\exp(-2|\alpha|^2)\cos(\varphi)]$) through a beam splitter with a second vacuum input such that the output modes are given by Eq. (21). Yurke and Stoler [28] have considered this situation to show that the output state is the two-mode cat state

$$|\mathrm{out}\rangle=N(|\sqrt{\eta}\alpha\rangle_c|\sqrt{1-\eta}\alpha\rangle_d+e^{i\varphi}|-\sqrt{\eta}\alpha\rangle_c|-\sqrt{1-\eta}\alpha\rangle_d). \tag{29}$$

We evaluate the relevant probability distributions $P_{\theta,\phi}(x,y)$ for measurement of X_θ^A and X_ϕ^B for the two-mode superposition state (26),

$$P_{\theta,\phi}(x,y)=\frac{\mathcal{A}}{2\pi}\sum_{L,R=-1}^{+1}K_{LR}\exp\left\{-\frac{1}{2}[x_\theta+\zeta_{LR}^{A,\theta}]^2\right\}\times\exp\left\{-\frac{1}{2}[x_\phi+\zeta_{LR}^{B,\phi}]^2\right\}, \tag{30}$$

where in the above equation L and R index four terms with L and R taking on the values ±1 and K_{LR} is defined as

$$K_{LR}=\exp\{(LR-1)(|\alpha_0|^2+|\beta_0|^2+Ri\varphi/2)\} \tag{31}$$

and the variable $\zeta_{LR}^{A,\theta}=-(R\alpha_0e^{-i\theta}+L\alpha_0^*e^{i\theta})$ has been introduced to simplify the notation. The variable $\zeta_{LR}^{B,\phi}$ for the other mode can be obtained simply by replacing α_0 and θ by β_0 and ϕ, respectively.

The event probabilities (20) can then be written in terms of error functions, for example, as

$$P_{++}^{AB}(\theta,\phi)=\frac{\mathcal{A}}{4}\sum_{L,R=-1}^{+1}E_{LR}^A(\theta)E_{LR}^B(\phi)K_{LR}. \tag{32}$$

Here $E_{LR}^A(\theta)=\mathrm{erfc}(\zeta_{LR}^{A,\theta}/\sqrt{2})$ [and similarly for $E_{LR}^B(\phi)$ but replacing A with B] has been introduced as shorthand for the complementary error function of a particular argument.

Using techniques [30] allowing calculation of the error functions with imaginary arguments we conduct a numerical search over all angles for a violation of the inequality (6). We found no violation, however.

VI. CONTRADICTION WITH LOCAL REALISM FOR QUADRATURE PHASE AMPLITUDE MEASUREMENTS ON A ''SQUEEZED TWO-MODE CAT'' STATE

In order to improve chances of observing both EPR correlations and contradiction with local hidden variables we consider the two-mode superposition state evolved under the action of a two-mode squeezing operator, corresponding physically to interaction with a nondegenerate parametric amplifier or equivalent system generating photon pairs. Thus we consider interactions given by the interaction Hamiltonian,

$$H_I=i\hbar\kappa(\hat{a}^\dagger\hat{b}^\dagger-\hat{a}\hat{b}). \tag{33}$$

A. EPR correlations for the squeezed cat state

It can be shown that such an evolution will generate EPR correlated beams $\hat{a}$ and $\hat{b}$, in the sense of the original EPR argument [1,10]. We define the following particular quadra-

ture phase amplitudes for modes $\hat{a}$ and $\hat{b}$: $\hat{X}_a=\hat{a}+\hat{a}^\dagger$ and $\hat{P}_a=(\hat{a}-\hat{a}^\dagger)/i$, and similar definitions for the mode $\hat{b}$. Now the solutions for the operators after a time t are

$$\hat{a}(t)=\hat{a}\cosh(\kappa t)+\hat{b}\sinh(\kappa t),$$
$$\hat{b}(t)=\hat{b}\cosh(\kappa t)+\hat{a}\sinh(\kappa t), \tag{34}$$

and for the quadrature phase operators

$$\hat{X}_a(t)=\hat{X}_a(0)\cosh(\kappa t)+\hat{X}_b(0)\sinh(\kappa t),$$
$$\hat{X}_b(t)=\hat{X}_b(0)\cosh(\kappa t)+\hat{X}_a(0)\sinh(\kappa t),$$
$$\hat{P}_a(t)=\hat{P}_a(0)\cosh(\kappa t)-\hat{P}_b(0)\sinh(\kappa t), \tag{35}$$
$$\hat{P}_b(t)=\hat{P}_b(0)\cosh(\kappa t)-\hat{P}_a(0)\sinh(\kappa t).$$

As κt increases $\hat{X}_a(t)$ becomes increasingly correlated with $\hat{X}_b(t)$ and $\hat{P}_a(t)$ becomes increasingly correlated with $-\hat{P}_b(t)$, with the correlation becoming perfect in the limit $\kappa T\rightarrow\infty$. With modes $\hat{a}$ and $\hat{b}$ spatially separated after interaction, this has been shown by one of us [10] to give a direct example of EPR correlations.

We can make two spatially separated measurements of the correlated quantities in each mode. The results can be subtracted, yielding an estimate of the error in inferring the value at A from a measurement at B. That is, we calculate $\delta_x=\hat{X}_a(t)-\gamma\hat{X}_b(t)$ and $\delta_p=\hat{P}_a(t)+\gamma\hat{P}_b(t)$ [10]. The factor γ is a simple amplification factor which we shall modify to give the best estimate possible (the minimum error). Over an ensemble of measurements we can calculate the variances associated with our inference of $\hat{X}_a$ from $\hat{X}_b$, and $\hat{P}_a$ from $\hat{P}_b$: $\Delta_x^2=\langle\delta_x^2\rangle-\langle\delta_x\rangle^2$ and $\Delta_p^2=\langle\delta_p^2\rangle-\langle\delta_p\rangle^2$.

The minimum variance will occur for a particular value of γ. Hence finding the local turning point with γ yields

$$\Delta_{x,\min}^2=\frac{\Delta\hat{X}_a(T)^2\Delta\hat{X}_b(T)^2-[\langle\hat{X}_a(T),\hat{X}_b(T)\rangle]^2}{\Delta\hat{X}_b(T)^2}, \tag{36}$$

where we have a similar expression for $\Delta_{p,\min}^2$ and the covariance is $\langle x,y\rangle=\langle xy\rangle-\langle x\rangle\langle y\rangle$. We can calculate the necessary averages for the two-mode ''cat'' state using the equations of motion. It is then easy to calculate the minimum variance product and this is illustrated in Fig. 6. As can be seen from the figure, we predict that the product $\Delta_{x,\min}^2\Delta_{p,\min}^2$ drops below the quantum limit ($\Delta_x^2\Delta_p^2<1/g^4$) illustrating EPR correlations.

B. Contradiction with local realism

In order to search for a violation of the Bell inequality, we must calculate the probability distributions for the results of the two quadrature phase amplitude measurements at locations A and B. One may use the same techniques as used above for the pair-coherent state. To give some visual information, however, we choose here to perform the calculation by first calculating the Wigner function, which is easily evaluated. The density operator for the system is

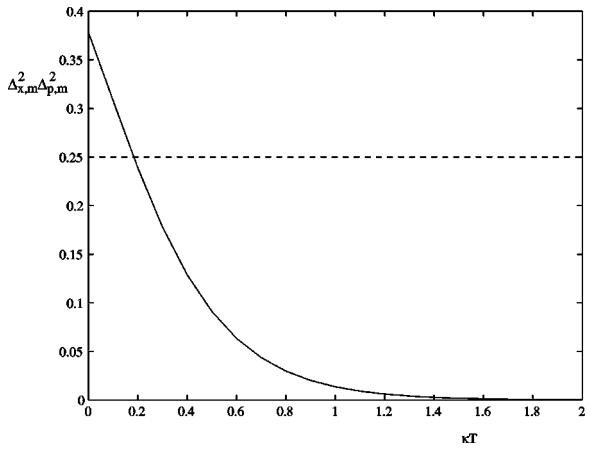

FIG. 6. The product of the minimum inference variances $\Delta_{x,\min}^2\Delta_{p,\min}^2$ for the ''squeezed'' two-mode ''cat'' state. The EPR incompleteness argument can be formulated when this product drops below $1/g^4$ (dashed line). The parameters are $\alpha_0=\beta_0=0.9$, $\varphi=0$, and $g=\sqrt{2}$.

$$\rho(t)=\hat{N}|\mathrm{cat}\rangle\langle\mathrm{cat}|\hat{N}^\dagger. \tag{37}$$

We write this as, recalling L and R take the values $+1$ or -1,

$$\rho(t)=\mathcal{A}\sum_{L,R=-1}^{+1}e^{(LR-1)Ri\varphi/2}\hat{N}\hat{D}(R\boldsymbol{\alpha}_0)|\mathbf{0}\rangle\langle\mathbf{0}|\hat{D}^\dagger(L\boldsymbol{\alpha}_0)\hat{N}^\dagger, \tag{38}$$

where

$$\hat{D}(\boldsymbol{\alpha}_0)=\exp(\alpha_0\hat{a}^\dagger-\alpha_0^*\hat{a}+\beta_0\hat{b}^\dagger-\beta_0^*\hat{b}),$$
$$\hat{N}=\exp(-i\hat{H}_It/\hbar).$$

The symmetric characteristic function is

$$\chi_s(\eta_1,\eta_2)=\mathrm{Tr}\{\rho(t)e^{\eta_1\hat{a}^\dagger-\eta_1^*\hat{a}+\eta_2\hat{b}^\dagger-\eta_2^*\hat{b}}\}=\mathcal{A}\sum_{L,R=-1}^{+1}\chi_{LR}, \tag{39}$$

where

$$\chi_{LR}=\langle\mathbf{L}\boldsymbol{\alpha}_\mathbf{0}|\hat{N}^\dagger\exp(\eta_1\hat{a}^\dagger-\eta_1^*\hat{a}+\eta_2\hat{b}^\dagger-\eta_2^*\hat{b})\hat{N}|\mathbf{R}\boldsymbol{\alpha}_\mathbf{0}\rangle \times e^{(LR-1)Ri\varphi/2}. \tag{40}$$

Now, since $\hat{N}$ is a unitary operator

$$\chi_{LR}=\langle\mathbf{L}\boldsymbol{\alpha}_\mathbf{0}|\exp[\eta_1\hat{a}(t)^\dagger-\eta_1^*\hat{a}(t)+\eta_2\hat{b}(t)^\dagger - \eta_2^*\hat{b}(t)]|\mathbf{R}\boldsymbol{\alpha}_\mathbf{0}\rangle e^{(LR-1)Ri\varphi/2}, \tag{41}$$

where the operators $\hat{a}(t)$ and $\hat{b}(t)$ are given by the equations of motion (34). Normally ordering the products in the exponential yields

$$\chi_{LR}=\exp\left\{-\frac{1}{2}\eta^\dagger\mathbf{A_1}\eta-\eta^\dagger\mathbf{X_{LR}}+\mathbf{X_{RL}}^\dagger\eta\right\}K_{LR}, \tag{42}$$

where

$$\eta=(\eta_1,-\eta_2^*)^T,$$

$$\mathbf{X_{LR}}=\begin{pmatrix} R\cosh(\kappa t)\alpha_0+ & L\sinh(\kappa t)\beta_0^* \\ L\cosh(\kappa t)\beta_0^*+ & R\sinh(\kappa t)\alpha_0 \end{pmatrix},$$

$$\mathbf{A_1}=\begin{pmatrix} \cosh(2\kappa t) & \sinh(2\kappa t) \\ \sinh(2\kappa t) & \cosh(2\kappa t) \end{pmatrix}.$$

The Wigner function is the Fourier transform of the characteristic function:

$$W=\mathcal{A}\sum_{L,R=-1}^{+1} W_{LR}, \tag{43}$$

$$W_{LR}=\frac{1}{\pi^4}\int d^2\eta e^{-\mathbf{X}^\dagger\eta+\eta^\dagger\mathbf{X}}\chi_{LR}, \tag{44}$$

with $\mathbf{X}=(\alpha,\beta^*)^T$. We can use the result for Gaussian integrals

$$\begin{aligned} I&=\int d^2\eta\exp(-\lambda\,\eta^\dagger\mathbf{A}\eta+\eta^\dagger\mathbf{x}_1+\mathbf{x}_2^\dagger\eta) \\ &=|\mathbf{A}|^{-1}\left(\frac{\pi}{\lambda}\right)^D\exp\left(\frac{1}{\lambda}\mathbf{x}_2^\dagger\mathbf{A}^{-1}\mathbf{x}_1\right), \end{aligned} \tag{45}$$

where D is the dimension of the vectors to evaluate the integrals, yielding

$$W_{LR}=\frac{4K_{LR}}{\pi^2}\exp\{-2(\mathbf{X}-\mathbf{X}_{RL})^\dagger\mathbf{A}_2(\mathbf{X}-\mathbf{X}_{LR})\}, \tag{46}$$

where

$$\mathbf{A}_2=\mathbf{A}_1^{-1}=\begin{pmatrix} \cosh(2\kappa t) & -\sinh(2\kappa t) \\ -\sinh(2\kappa t) & \cosh(2\kappa t) \end{pmatrix}. \tag{47}$$

Now, we can introduce new variables x and p such that $\alpha=(x_a+ip_a)/2$ and $\beta=(x_b+ip_b)/2$. Using the vectors $\mathbf{x}=(x_a,x_b)^T$ and $\mathbf{p}=(p_a,-p_b)^T$, together with $\mathbf{x}_0=(\mathbf{X}_{LR}+\mathbf{X}_{RL}^*)/g$ and $\mathbf{p}_0=(\mathbf{X}_{LR}-\mathbf{X}_{RL}^*)/gi$, Eq. (46) then becomes

$$\begin{aligned} W_{LR}=\frac{g^4K_{LR}}{4\pi^2}\exp\Big\{&-\frac{g^2}{2}(\mathbf{x}-\mathbf{x}_0)^T\mathbf{A}_2(\mathbf{x}-\mathbf{x}_0) \\ &-\frac{g^2}{2}(\mathbf{p}-\mathbf{p}_0)^T\mathbf{A}_2(\mathbf{p}-\mathbf{p}_0)\Big\}. \end{aligned} \tag{48}$$

Setting $\kappa T=0$ gives the Wigner function for the two-mode cat state, plotted in Fig. 7. We observe the presence of fringes and note the function is negative. The figure illustrates the effect of increasing κT. Note that the Wigner function remains negative, preventing the interpretation of the Wigner function as a direct hidden variable theory.

In the limit of large interaction time where $\cosh(\kappa t)\approx\sinh(\kappa t)$ then

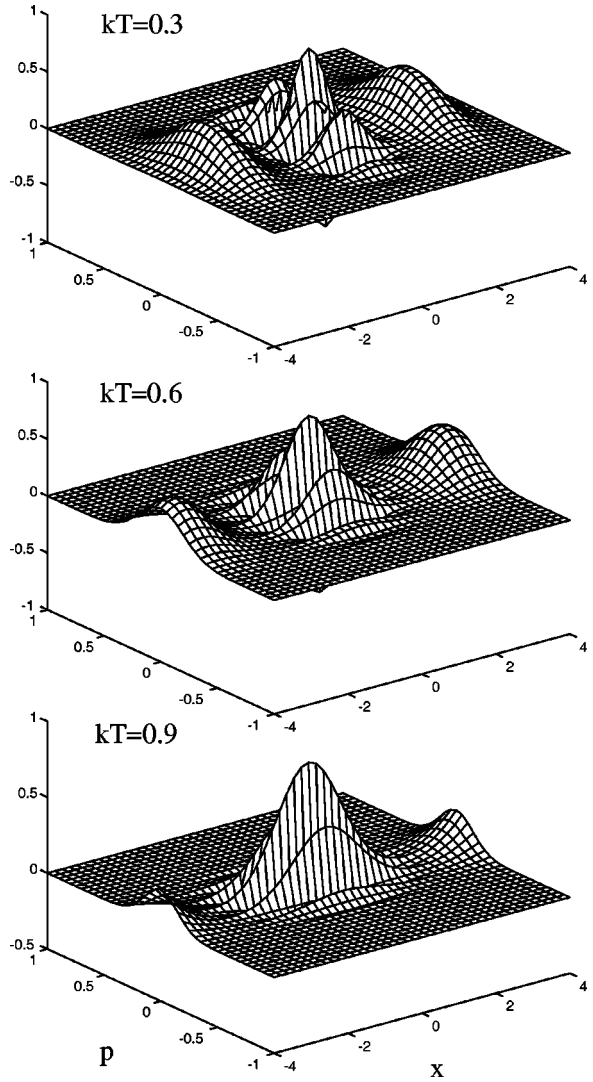

FIG. 7. Wigner function plotted with $x_a=x_b=x$ and $p_a=p_b=p$ and $\varphi=0$ for an initial two-mode ''cat'' state with $\alpha_0=\beta_0=2$.

$$\mathbf{x}_0=\frac{2\cosh(\kappa t)}{g}\mathrm{Re}(R\alpha_0+L\beta_0)\begin{pmatrix}1\\1\end{pmatrix},$$

$$\mathbf{p}_0=\frac{2\cosh(\kappa t)}{g}\mathrm{Im}(R\alpha_0-L\beta_0)\begin{pmatrix}1\\1\end{pmatrix},$$

where here Re and Im refer to real and imaginary parts. Both of these expressions are real, and hence there are no complex terms in W_{LR} that can lead to oscillations. Here W_{LR} becomes a Gaussian and is everywhere positive, and can act as a local hidden variable theory for quadrature phase measurements. We conclude therefore that no contradiction of local realism for our proposed experiment will occur in this limit.

We introduce the following variables to include a homodyne measurement at an arbitrary phase angle. That is, we start from Eq. (46) but introduce the more general x_θ, x_ϕ, p_θ and p_ϕ: $\alpha=e^{i\theta}(x_\theta+ip_\theta)/2$ and $\beta=e^{i\phi}(x_\phi+ip_\phi)/2$. We define the vectors $\mathbf{x}=(x_\theta,x_\phi)^T$, $\mathbf{p}=(p_\theta,-p_\phi)^T$. Now we obtain

$$W_{LR}=\frac{g^4K_{LR}}{4\pi^2}\exp\left\{-\frac{g^2}{2}\left(\mathbf{x}+i\mathbf{p}-\frac{2}{g}\mathbf{X}_{RL}\right)^{\dagger}\times\mathbf{A}_3\left(\mathbf{x}+i\mathbf{p}-\frac{2}{g}\mathbf{X}_{LR}\right)\right\}, \tag{49}$$

with

$$\mathbf{A}_3=\mathbf{E}^{\dagger}\mathbf{A}_2\mathbf{E}=\begin{pmatrix}\cosh(2\kappa t) & -\sinh(2\kappa t)e^{-i(\theta+\phi)}\\ -\sinh(2\kappa t)e^{i(\theta+\phi)} & \cosh(2\kappa t)\end{pmatrix} \tag{50}$$

and

$$\mathbf{E}=\begin{pmatrix}e^{i\theta} & 0\\ 0 & e^{-i\phi}\end{pmatrix}. \tag{51}$$

We need to integrate out the **p** terms as this will yield $P_{\theta,\phi}(x,y)$:

$$P_{\theta,\phi}(x,y)=\int d\mathbf{p}W,$$
$$P_{\theta,\phi}(x,y)=\sum_{L,R=-1}^{+1}P_{\theta,\phi}(x,y)_{LR}. \tag{52}$$

Now, expanding out Eq. (49) and integrating over p_θ followed by p_ϕ leads to a messy expression which, after some work, can be simplified as

$$P_{\theta,\phi}(x,y)_{LR}=\frac{g^2K_{LR}}{2\pi\sqrt{\mathcal{C}}}\exp\left\{-\frac{g^2}{2}\mathbf{x}^T\mathbf{A}_4^{-1}\mathbf{x}+\mathbf{R}^T\mathbf{x}+G\right\}$$
$$=\frac{g^2K_{LR}}{2\pi\sqrt{\mathcal{C}}}\exp\{-a(x_\theta^2+x_\phi^2)+2bx_\theta x_\phi+R_1x_\theta+R_2x_\phi+G\}, \tag{53}$$

where

$$\mathcal{C}=\cosh(2\kappa t)^2-\sinh(2\kappa t)^2\cos(\theta+\phi),$$

$$\mathbf{A}_4=\begin{pmatrix}\cosh(2\kappa t) & \sinh(2\kappa t)\cos(\theta+\phi)\\ \sinh(2\kappa t)\cos(\theta+\phi) & \cosh(2\kappa t)\end{pmatrix},$$

$$\mathbf{R}=g(\mathbf{A}_3\tilde{\mathbf{X}}_{LR}+\mathbf{A}_3^T\tilde{\mathbf{X}}_{RL}^*)-\frac{g}{2\mathcal{C}}(\mathbf{A}_3-\mathbf{A}_3^T)\mathbf{A}_4(\mathbf{A}_3\tilde{\mathbf{X}}_{LR}-\mathbf{A}_3^T\tilde{\mathbf{X}}_{RL}^*),$$

$$G=\frac{-1}{2\mathcal{C}}(\mathbf{A}_3\tilde{\mathbf{X}}_{LR}-\mathbf{A}_3^T\tilde{\mathbf{X}}_{RL}^*)^T\mathbf{A}_4(\mathbf{A}_3\tilde{\mathbf{X}}_{LR}-\mathbf{A}_3^T\tilde{\mathbf{X}}_{RL}^*)-2\tilde{\mathbf{X}}_{RL}^{\dagger}\mathbf{A}_3\tilde{\mathbf{X}}_{LR},$$

$$\tilde{\mathbf{X}}_{LR}=\mathbf{E}^{-1}\mathbf{X}_{LR},$$

$$a=g^2\cosh(2\kappa t)/2\mathcal{C},$$

$$b=g^2\sinh(2\kappa t)\cos(\theta+\phi)/2\mathcal{C}.$$

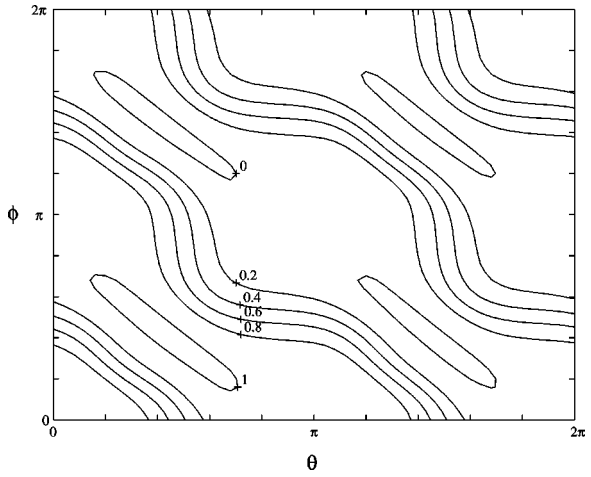

FIG. 8. The violation of the CH-Bell inequality found for a squeezed two-mode ''cat'' state. A contour plot of S that contains the maximum violation found. Parameters $\alpha_0=\beta_0=0.9$, $\kappa t=0.6$, $\varphi=0$, and $\delta=0.7\pi$. The maximum achieved violation is $S=1.008$ at $\theta=\phi=0.42\pi$.

Now, finally, we integrate over a quadrant of the two-dimensional Gaussian to get the joint probability of detecting a $(+)$ result at A and a $(+)$ result at B.

$$P_{++}^{AB}(\theta,\phi)=\sum_{L,R=-1}^{+1}P_{++}^{AB}(\theta,\phi)_{LR},$$

$$P_{++}^{AB}(\theta,\phi)_{LR}=\int_0^{\infty}dx_\theta\int_0^{\infty}dx_\phi P_{\theta,\phi}(x,y)_{LR}. \tag{54}$$

We may integrate this directly by numerical integration. Alternatively some work (Appendix C) allows for expressions which may be evaluated more readily by numerical techniques allowing for a search with a wide range of angles. The main obstacle to finding a violation is the large size of parameter space that needs to be searched. The full CH-Bell inequality depends on values of α_0, β_0, κt, and φ. Again it is useful do define the angles $\delta_1=\theta-\theta'$ and $\delta_2=\phi'-\phi$. A quick search reveals that the maximum value of our CH-Bell inequality always seems to occur for $\delta_1=\delta_2$. In order to reduce the size of the search of parameter space, we will take $\delta_1=\delta_2$ in the following calculations. Given $\delta_1=\delta_2=\delta$, the CH-Bell inequality can be reduced to a three-angle form: $S(\theta,\phi,\delta)$. We shall also assume that $\alpha_0=\beta_0$ and further that this value is a real number.

With these restrictions a preliminary search of parameter space does indeed find a violation, with the ''best'' value occurring for the parameters $\alpha_0=\beta_0=0.9$ and $\kappa t=0.6$.

Exploring the behavior of the maximum of $S(\theta,\phi,\delta)$ with φ shows the behavior that seems independent of the other parameters. In this search the domains of θ, ϕ, δ, and φ were divided into 50 points.

Henceforth we will choose $\varphi=0$. Examining the behavior with δ also gives a preferred value for this parameter, with $\delta=0.7\pi$.

Finally we are in a position to plot $S(\theta,\phi)$ and this is performed in Figs. 8 and 9, which show a region where the

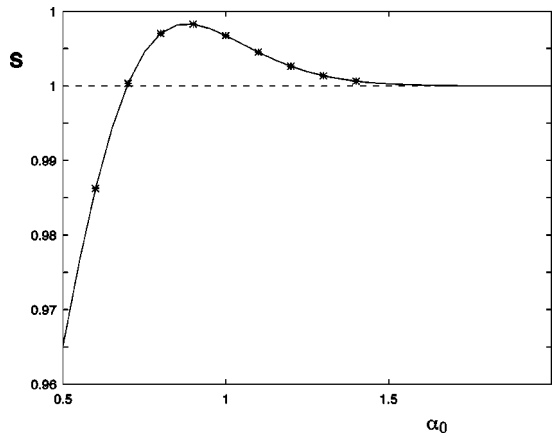

FIG. 9. The violation of the CH-Bell inequality found for the squeezed two-mode ''cat'' state. The behavior of S with α_0 (note that $\alpha_0=\beta_0$). The parameters are $\kappa t=0.6$, $\varphi=0$, $\theta=\phi=0.42\pi$, and $\delta=0.7\pi$.

violation occurs. The maximum value reached is $S=1.008$ at $\theta=\phi=0.42\pi$.

Now we can examine the behavior with α_0 in more detail. This is depicted in Fig. 9. Notice that S rapidly approaches one so that the violation is for a small parameter range only. Note also that S seems to approach one asymptotically from above, seeming to imply that a macroscopically sized superposition state would also violate the CH-Bell inequality (though by a tiny amount).

VII. CONCLUSION

We have expanded on our previous publication to present two quantum systems which give a violation with local realism for experiments involving only quadrature phase amplitude (position and momentum) measurements. A small but conclusive deviation from a Bell inequality has been found for a pair-coherent state and a suitably squeezed superposition of two two-mode coherent states. The effect of detection inefficiency and loss on the violation has been calculated (transmission of order 95% required). While such efficiencies may be obtainable by the homodyne detection procedure, this sensitivity to loss may hinder the generation of the suitable quantum state.

ACKNOWLEDGMENTS

We are grateful to C. W. Gardiner and W. J. Munro for many helpful suggestions.

APPENDIX A

Provided we can interchange the order of integration and complete the square, we write, using the result (18), Eq. (20) as

$$P_{++}^{AB}(\theta,\phi)=\frac{\mathcal{B}}{4}\int_0^{2\pi}d\vartheta\int_0^{2\pi}d\vartheta' \times\exp\{2r_0^2[\cos(\vartheta-\vartheta')-1]\}\mathrm{erfc}(A)\mathrm{erfc}(B). \tag{A1}$$

Similarly we can construct [note that we must have $P_+^B(\phi)=P_+^A(\phi)$ from the symmetry of the pair-coherent state under interchange of $\hat{a}$ with $\hat{b}$]

$$P_+^A(\theta)=\frac{\mathcal{B}}{2}\int_0^{2\pi}d\vartheta\int_0^{2\pi}d\vartheta' \times\exp\{2r_0^2[\cos(\vartheta-\vartheta')-1]\}\mathrm{erfc}(A). \tag{A2}$$

We will employ a power series expansion for the error functions:

$$\mathrm{erf}(k[e^{ia}+e^{-ia'}])=\frac{2}{\sqrt{\pi}}\sum_{n=0}^{\infty}\sum_{r=0}^{2n+1}\frac{(-1)^n k^{2n+1}(2n)!}{n!r!(2n+1-r)!} \times e^{iu(2n+1-r)}e^{ia(2r-2n-1)}, \tag{A3}$$

where we have also used the binomial expansion and the substitution $a'=a-u$. Note the following result which arises when integrating the above expression:

$$\int_0^{2\pi}da\,\mathrm{erf}(k[e^{ia}+e^{-ia'}])=\sum_{n,r}(\ldots)\int_0^{2\pi}da e^{ia(2r-2n-1)} =\sum_{n,r}(\ldots)2\pi\delta_{r,n+1/2}=0, \tag{A4}$$

where $(\ldots)$ denotes the terms in Eq. (A3) that are not explicitly written. This result follows since both r and n are integral values and the delta function $\delta_{r,n+1/2}$ will always be zero.

Now we have

$$P_+^A(\theta)=\frac{\mathcal{B}e^{-2r_0^2}}{2}\int_0^{2\pi}d\vartheta\int_0^{2\pi}d\vartheta' e^{2r_0^2\cos(\vartheta-\vartheta')} \times\left\{1-\mathrm{erf}\left(-\frac{r_0}{\sqrt{2}}[e^{i(\vartheta-\chi)}+e^{-i(\vartheta'-\chi)}]\right)\right\}. \tag{A5}$$

With a change of variables to $a=\vartheta-\chi$ and $a'=a-u$, where $u=\vartheta-\vartheta'$, it is evident that because of Eq. (A4), the integral over the error function vanishes, leaving an integral that can be identified as a Bessel function:

$$P_+^A(\theta)=\frac{\mathcal{B}e^{-2r_0^2}}{2}(2\pi)^2 I_0(2r_0^2)=\frac{1}{2}. \tag{A6}$$

Now, $P_{++}^{AB}(\theta,\phi)$ can be treated in a similar way.

$$P_{++}^{AB}(\theta,\phi)=\frac{\mathcal{B}e^{-2r_0^2}}{4}\int_0^{2\pi}d\vartheta\int_0^{2\pi}d\vartheta' e^{2r_0^2\cos(\vartheta-\vartheta')} \times\{1-\mathrm{erf}(A)-\mathrm{erf}(B)+\mathrm{erf}(A)\mathrm{erf}(B)\} \tag{A7}$$

and it can be seen that the first term will give a value of $\frac{1}{4}$, the next two terms will vanish, and the last term is the only one that will present any difficulty. Hence we can write

$$P_{++}^{AB}(\theta,\phi)=\frac{1}{4}+F(\mathrm{erf}(A)\mathrm{erf}(B)) \tag{A8}$$

and F is the function left after dropping the first three terms in Eq. (A7). As before, each of the terms in the product $\mathrm{erf}(A)\mathrm{erf}(B)$ can be expanded in a power series, yielding

$$\begin{aligned}\mathrm{erf}(A)\mathrm{erf}(B)=&\frac{4k^2}{\pi}\sum_{n=0}^{\infty}\sum_{m=0}^{\infty}\sum_{r=0}^{2n+1}\sum_{p=0}^{2m+1}\\&\times f(n,m,r,p)(-k^2)^{m+n}\\&\times e^{iu(2n-r+p-2m)}e^{2i\vartheta(r-n+m-p)}\\&\times e^{-i\chi(2r-2n-1)},\end{aligned} \tag{A9}$$

$$f(n,m,r,p)=\frac{(2n)!(2m)!}{n!m!r!p!(2n+1-r)!(2m+1-p)!}, \tag{A10}$$

where $k=-r_0/\sqrt{2}$ and the variable change of $\vartheta'=\vartheta-u$ has been utilized.

The integrals will now yield a Kronecker δ function and a modified Bessel function:

$$\begin{aligned}F=&\frac{\mathcal{B}e^{-2r_0^2}k^2}{\pi}\sum_{n,m,r,p}f(n,m,r,p)e^{-i\chi(2r-2n-1)}\\&\times\int_0^{2\pi}du e^{2r_0^2\cos(u)}e^{iu(2n-r+p-2m)}\int_0^{2\pi}d\vartheta e^{2i\vartheta(r-n+m-p)}\end{aligned} \tag{A11}$$

$$\begin{aligned}=&4\pi\mathcal{B}e^{-2r_0^2}k^2\sum_{n,m,r,p}f(n,m,r,p)\\&\times e^{-i\chi(2r-2n-1)}\delta_{m-p,n-r}I_{2(n-m)+p-r}(2r_0^2).\end{aligned} \tag{A12}$$

Utilizing the δ function by setting $p=m-n+r$ on the understanding that the factorial sequences terminate at zero, we can write

$$\begin{aligned}F=&4\pi\mathcal{B}e^{-2r_0^2}k^2\sum_{n=0}^{\infty}\sum_{m=0}^{\infty}\sum_{r=0}^{2n+1}f(n,m,r)(-k^2)^{m+n}\\&\times I_{n-m}(2r_0^2)e^{-i\chi(2r-2n-1)},\end{aligned} \tag{A13}$$

$$\begin{aligned}&f(n,m,r)\\&=\frac{(2n)!(2m)!}{n!m!r!(r+m-n)!(n+m-r+1)!(2n+1-r)!}.\end{aligned} \tag{A14}$$

We can now change variables in the summations to $s=2r-2n-1$. Truncating the n and m summations at some value M will yield

$$F=4\pi\mathcal{B}e^{-2r_0^2}k^2\sum_{s=-(2M+1),\,s\ \mathrm{odd}}^{2M+1}\mathbf{X}_s e^{-i\chi s}, \tag{A15}$$

where $\mathbf{X}_s$ is a vector of values indexed by s and given explicitly as

$$\begin{aligned}\mathbf{X}_s=&\sum_{n=|s/2|-1/2}^{M}\sum_{m=|s/2|-1/2}^{M}f\left(n,m,\frac{s+2n+1}{2}\right)\\&\times I_{n-m}(2r_0^2)(-k^2)^{n+m}.\end{aligned} \tag{A16}$$

Equation (A15) is the definition of a discrete Fourier transform so by using the fast Fourier transform we can evaluate this expression very quickly.

APPENDIX B

In the limit of large r_0 the exponent in Eq. (A1) becomes the delta function $\delta(\vartheta-\vartheta')$:

$$\lim_{r_0\to\infty}\int_0^{2\pi}d\vartheta'\exp\{2r_0^2[\cos(\vartheta-\vartheta')-1]\}=\frac{\sqrt{\pi}}{r_0}\delta(\vartheta-\vartheta') \tag{B1}$$

in which case performing the ϑ' integrals we get

$$\begin{aligned}P_{++}^{AB}(\theta,\phi)=&\frac{\sqrt{\pi}\mathcal{B}}{4r_0}\int_0^{2\pi}d\vartheta\,\mathrm{erfc}[-\sqrt{2}r_0\cos(\vartheta-\chi)]\\&\times\mathrm{erfc}[-\sqrt{2}r_0\cos(\vartheta)],\end{aligned} \tag{B2}$$

$$P_{+}^{A}(\theta)=\frac{\sqrt{\pi}\mathcal{B}}{2r_0}\int_0^{2\pi}d\vartheta\,\mathrm{erfc}[-\sqrt{2}r_0\cos(\vartheta-\chi)]. \tag{B3}$$

For large r_0, $\mathrm{erfc}[-\sqrt{2}r_0\cos(\vartheta-\chi)]$ acts like a step function and hence we can evaluate the remaining integrals. Noting that for large r_0 the normalization constant evaluates to $\mathcal{B}^{-1}=2\pi\sqrt{\pi}/r_0$ we get

$$P_{++}^{AB}(\theta,\phi)=\left|\frac{1}{2}-\frac{(\theta+\phi)\bmod 2\pi}{2\pi}\right|, \tag{B4}$$

$$P_{+}^{A}(\theta)=P_{+}^{B}(\phi)=1/2. \tag{B5}$$

APPENDIX C

In order to evaluate the expression $P_{++}^{AB}(\theta,\phi)$ we rotate the axis by $\pi/4$, then scale the axis, and finally change to polar coordinates: $(x_\theta+x_\phi)\sqrt{(a-b)/2}=r\cos\omega$ and $(x_\theta-x_\phi)\sqrt{(a+b)/2}=r\sin\omega$. With this transformation we arrive at

$$P_{++}^{AB}(\theta,\phi)_{LR}=\frac{K_{LR}}{\pi}\int_0^{\infty}dr\,r\int_{-\omega_0}^{\omega_0}d\omega e^{-r^2}e^{r(A\cos\omega+B\sin\omega)}, \tag{C1}$$

where $\omega_0=\tan^{-1}[\sqrt{(a+b)/(a-b)}]$. Using a power series expansion will give

$$P_{++}^{AB}(\theta,\phi)_{LR}=\frac{K_{LR}}{\pi}\sum_{n=0}^{\infty}\int_0^{\infty}dr\,\frac{r^{n+1}e^{-r^2}}{n!}\times\int_{-\omega_0}^{\omega_0}d\omega\left[\left(\frac{A-iB}{2}\right)e^{i\omega}+\left(\frac{A+iB}{2}\right)e^{-i\omega}\right]^n, \tag{C2}$$

where

$$A=(R_1+R_2)/\sqrt{2[\cosh(2\kappa t)+\sinh(2\kappa t)\cos(\theta+\phi)]},$$

$$B=(R_1-R_2)/\sqrt{2[\cosh(2\kappa t)-\sinh(2\kappa t)\cos(\theta+\phi)]}.$$

The r integral in Eq. (C2) gives a gamma function Γ, while the ω expression can be further expanded as a binomial series, and upon integration gives

$$P_{++}^{AB}(\theta,\phi)_{LR}=\frac{K_{LR}}{\pi}\sum_{n=0}^{\infty}\sum_{r=0}^{n}\frac{\Gamma(n/2+1)A_2^rB_2^{n-r}}{(n-r)!r!}\times\begin{cases}\dfrac{\sin(\omega_0[2r-n])}{(2r-n)}, & 2r\neq n\\ \omega_0, & 2r=n\end{cases} \tag{C3}$$

where $A_2=(A-iB)/2$ and $B_2=(A+iB)/2$.

Calculating $P_+^A(\theta)$ and $P_+^B(\phi)$ is a straightforward modification of the previous calculation. Performing the integrations yields, after some manipulation,

$$P_+^A(\theta)_{LR}=\frac{K_{LR}}{2}\mathrm{erfc}\left(\frac{-1}{\sqrt{2\cosh(2\kappa t)}}\mathbf{u}_1^T(\mathbf{E}\mathbf{X}_{RL}^*+\mathbf{E}^*\mathbf{X}_{LR})\right), \tag{C4}$$

$$P_+^B(\phi)_{LR}=\frac{K_{LR}}{2}\mathrm{erfc}\left(\frac{-1}{\sqrt{2\cosh(2\kappa t)}}\mathbf{u}_2^T(\mathbf{E}\mathbf{X}_{RL}^*+\mathbf{E}^*\mathbf{X}_{LR})\right), \tag{C5}$$

where $\mathbf{u}_1=(1,0)^T$ and $\mathbf{u}_2=(0,1)^T$.

[1] A. Einstein, B. Podolsky, and N. Rosen, Phys. Rev. **47**, 777 (1935).

[2] J. S. Bell, Physics (Long Island City, N.Y.) **1**, 195 (1965); *Speakable and Unspeakable in Quantum Mechanics* (Cambridge University Press, Cambridge, England, 1988); J. F. Clauser and A. Shimony, Rep. Prog. Phys. **41**, 1881 (1978), and references therein.

[3] A. Aspect, P. Grangier, and G. Roger, Phys. Rev. Lett. **49**, 91 (1982); A. Aspect, J. Dalibard, and G. Roger, *ibid.* **49**, 1804 (1982); Y. H. Shih and C. O. Alley, *ibid.* **61**, 2921 (1998); Z. Y. Ou and L. Mandel, *ibid.* **61**, 50 (1988); J. G. Rarity and P. R. Tapster, *ibid.* **64**, 2495 (1990); J. Brendel, E. Mohler, and W. Martienssen, Europhys. Lett. **20**, 575 (1992); P. G. Kwiat, A. M. Steinberg, and R. Y. Chiao, Phys. Rev. A **47**, R2472 (1993); T. E. Kiess, Y. H. Shih, A. V. Sergienko, and C. O. Alley, Phys. Rev. Lett. **71**, 3893 (1993); P. G. Kwiat, K. Mattle, H. Weinfurter, Z. Zeilinger, A. Sergienko, and Y. Shih, *ibid.* **75**, 4337 (1995); D. V. Strekalov, T. B. Pittman, A. V. Sergienko, Y. H. Shih, and P. G. Kwiat, Phys. Rev. A **54**, R1 (1996); W. Gregor, T. Jennewein, and A. Zeilinger, Phys. Rev. Lett. **81**, 5039 (1998).

[4] M. A. Horne, A. Shimony, and A. Zeilinger, Phys. Rev. Lett. **62**, 2209 (1989); M. D. Reid and D. F. Walls, Phys. Rev. A **34**, 1260 (1985); J. G. Rarity and P. R. Tapster, Phys. Rev. Lett. **64**, 2495 (1990); D. M. Greenberger, M. A. Horne, A. Shimony, and A. Zeilinger, Am. J. Phys. **58**, 1131 (1990).

[5] N. D. Mermin, Phys. Rev. D **22**, 356 (1980); P. D. Drummond, Phys. Rev. Lett. **50**, 1407 (1983); A. Garg and N. D. Mermin, *ibid.* **49**, 901 (1982); N. D. Mermin, *ibid.* **65**, 1838 (1990); S. M. Roy and V. Singh, *ibid.* **67**, 2761 (1991); A. Peres, Phys. Rev. A **46**, 4413 (1992); M. D. Reid and W. J. Munro, Phys. Rev. Lett. **69**, 997 (1992); G. S. Agarwal, Phys. Rev. A **47**, 4608 (1993); D. Home and A. S. Mujumdar, *ibid.* **52**, 4959 (1995); C. Gerry, *ibid.* **54**, R2529 (1996).

[6] D. M. Greenberger, M. Horne, and A. Zeilinger, in *Bell's Theorem, Quantum Theory and Conceptions of the Universe*, edited by M. Kafatos (Kluwer, Dordrecht, 1989), p. 69; N. D. Mermin, Phys. Today **43**, 9 (1990); D. M. Greenberger, M. A. Horne, A. Shimony, and A. Zeilinger, Am. J. Phys. **58**, 1131 (1990).

[7] J. F. Clauser and M. A. Horne, Phys. Rev. D **10**, 526 (1974).

[8] S. Pascazio, in *Quantum Mechanics versus Local Realism*, edited by F. Selleri (Plenum, New York, 1988), p. 391; E. Santos, Phys. Rev. A **46**, 3646 (1992); M. Ferrero, T. W. Marshall, and E. Santos, Am. J. Phys. **58**, 683 (1990); T. W. Marshall, E. Santos, and F. Selleri, Phys. Lett. **98A**, 5 (1983); T. Marshall and E. Santos, Phys. Rev. A **39**, 6271 (1989); E. Santos, Phys. Lett. A **139**, 431 (1989).

[9] A. Gilchrist, P. Deuar, and M. D. Reid, Phys. Rev. Lett. **80**, 3169 (1998).

[10] M. D. Reid, Phys. Rev. A **40**, 913 (1989).

[11] M. D. Reid, Europhys. Lett. **36**, 1 (1996); Quantum Semiclassic. Opt. **9**, 489 (1997); M. D. Reid and P. Deuar, Ann. Phys. (N.Y.) **265**, 52 (1998).

[12] Z. Y. Ou, S. F. Pereira, H. J. Kimble, and K. C. Peng, Phys. Rev. Lett. **68**, 3663 (1992).

[13] H. P. Yuen and X. Shapiro, IEEE Trans. Inf. Theory **26**, 78 (1980); H. P. Yuen and V. W. S. Chan, Opt. Lett. **8**, 177 (1983); B. Yurke, Phys. Rev. A **32**, 311 (1985); U. Leonhardt and H. Paul, Phys. Rev. Lett. **72**, 4086 (1994).

[14] P. Grangier, M. J. Potasek, and B. Yurke, Phys. Rev. A **38**, 3132 (1988); B. J. Oliver and C. R. Stroud, Phys. Lett. A **135**, 407 (1989); S. M. Tan, D. F. Walls, and M. J. Collett, Phys. Rev. Lett. **66**, 252 (1991); B. J. Sanders, Phys. Rev. A **45**, 6811 (1992).

[15] B. Yurke, M. Hillery, and D. Stoler, e-print quant-ph/9909042.

[16] W. J. Munro and G. J. Milburn, Phys. Rev. Lett. **81**, 4285 (1998).

[17] G. S. Agarwal, Phys. Rev. Lett. **57**, 827 (1986); J. Opt. Soc. Am. **5**, 1940 (1988); G. S. Agarwal, M. Graf, and M. Orszag, Phys. Rev. A **49**, 4077 (1994).
[18] K. Tara and G. S. Agarwal, Phys. Rev. A **50**, 2870 (1994).
[19] M. D. Reid and L. Krippner, Phys. Rev. A **47**, 552 (1993).
[20] V. V. Dodonov, I. A. Malkin, and V. I. Man'ko, Physica (Amsterdam) **72**, 597 (1974); Y. Xia and G. Guo, Phys. Lett. A **136**, 281 (1989); V. V. Dodonov, V. I. Man'ko, and D. E. Nikonov, Phys. Rev. A **51**, 3328 (1995).
[21] C. C. Gerry and E. E. Hatch III, Phys. Lett. A **174**, 185 (1993); E. E. Hatch III and C. C. Gerry, Phys. Rev. A **49**, 490 (1994); L. Gilles and P. L. Knight, *ibid.* **48**, 1582 (1993); L. Gilles, B. M. Garraway, and P. L. Knight, *ibid.* **49**, 2785 (1994).
[22] M. Wolinsky and H. Carmichael, Phys. Rev. Lett. **60**, 1836 (1988); H. J. Carmichael and M. Wolinsky, in *OSA Annual Meeting*, Technical Digest Vol. 18 (Optical Society of America, Washington, DC, 1989); L. Krippner, W. J. Munro, and M. D. Reid, Phys. Rev. A **50**, 4330 (1994); **52**, 2388 (1995).
[23] C. Monroe, D. M. Meekhof, B. E. King, and D. J. Wineland, Science **272**, 1131 (1996); M. Brune, E. Hagley, J. Dreyer, X. Maitre, A. Maali, C. Wunderlich, J. M. Raimond, and S. Haroche, Phys. Rev. Lett. **77**, 4887 (1996); M. W. Noel and C. R. Stroud, *ibid.* **77**, 1913 (1996).
[24] E. Schrödinger, Naturwissenschaften **23**, 812 (1935); V. Buzek and P. L. Knight, Prog. Opt. **34**, 1 (1995), and references therein.
[25] A. J. Leggett and A. Garg, Phys. Rev. Lett. **54**, 857 (1985); A. J. Leggett, in *Directions in Condensed Matter Physics*, edited by G. Grinstein and G. Mazenko (World Scientific, Singapore, 1986); W. H. Zurek, Phys. Today **44**, 236 (1991).
[26] A. Peres, *Quantum Theory: Concepts and Methods* (Kluwer Academic, Dordrecht, 1993).
[27] E. S. Polzik, J. Carri, and H. J. Kimble, Phys. Rev. Lett. **68**, 3020 (1992).
[28] B. Yurke and D. Stoler, Phys. Rev. Lett. **57**, 13 (1986).
[29] C. C. Gerry and R. Grobe, Phys. Rev. A **51**, 1698 (1995); N. A. Ansari and V. I. Man'ko, *ibid.* **50**, 1942 (1994).
[30] H. E. Salzer, Math. Tables Aids Comp. **5**, 67 (1951).